

Application of MSC/DYTRAN to the Hydrodynamic Ram Problem

Geetha Bharatram, Capt. Scott A. Schimmels, Dr. Vipperla B. Venkayya
Structures Division, Wright Laboratory
Wright Patterson AFB, Ohio 45433-7552

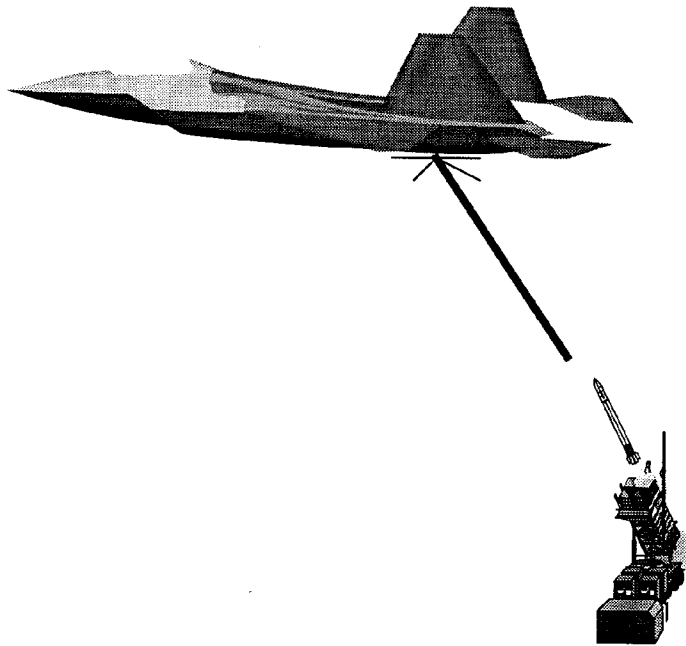
An analysis method for studying hydrodynamic ram effects in a fluid-filled structure is developed using MSC/DYTRAN. In this study a high velocity projectile is shot into a structure, depositing energy into the contained fluid and transmitting an impulse to the structure. The coupled fluid-structure interaction response is studied using MSC/DYTRAN. An Arbitrary Lagrange Euler (ALE) coupling is defined between the structure and the internal fluid and a general coupling is defined between the penetrating projectile and the fluid.

A second case is also studied, in which the penetrating projectile explodes at a predetermined time inside the fluid. Combined effects of the explosive blast and the hydrodynamic ram effects are studied. Preliminary results are presented in this paper.

1. Introduction

The hydrodynamic ram effect in fuel tanks is identified as one of the important factors in aircraft vulnerability. Hydrodynamic ram refers to the high pressures that are developed within a fluid when a high speed projectile penetrates a tank. The passage of the projectile through the fuel causes an intense pressure pulse to propagate in the fuel and strike the walls of the tank. This large internal fluid pressure on the walls causes severe petaling of the walls, usually at the entrance and exit points of the projectile.

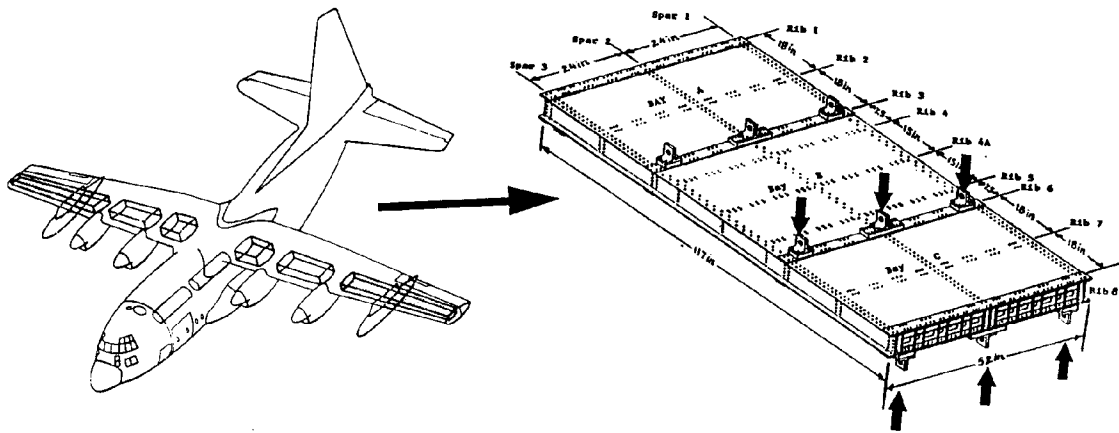
Hydrodynamic ram effects have proven to be a major combat related threat to the modern aircraft. Since the fuel tanks of tactical aircraft have the largest exposed area of all the vulnerable components, engineering estimates of fuel tank response to penetrating ballistic projectiles are required in order to design more survivable tanks. Figure 1 shows a possible threat on an aircraft from a surface-to-air missile.



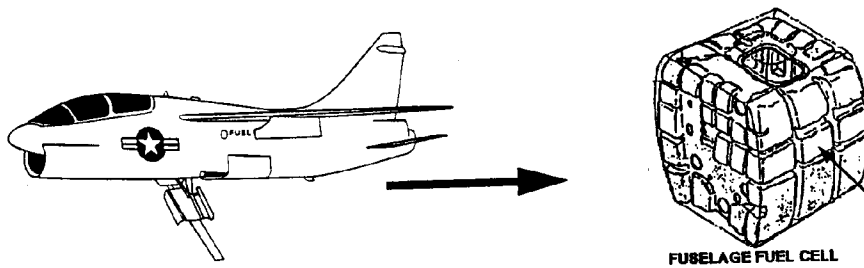
1. Missile Threat on an Airplane

Fuel tanks in cargo aircraft are generally wing integral fuel tanks as shown in Figure 2. The fuel cell is primarily the wing box [1]. The outer skin can either be metal or composite, depending on the wing skin composition. Fuselage integral fuel tanks are primarily found in fighter aircraft (Figure 3). Possible threats capable of producing Hydrodynamic Ram (HR) include: HEI (High Energy Incendiary), API (Armor Piercing Incendiary) or due to missile fragments. The HR effects can cause different aircraft failure modes such as engine kill (fuel injection), structural kill, or

other component kills (fire). The ballistic threat variables affecting HR damage are weight, shape, velocity, obliquity angle of the projectile and for the HEI projectile also the charge weight and detonation location. In the structural side thickness, layup, fiber/resin system are the issues affecting the extent of HR damage.



2. Wing Integral Fuel Tank



3. Fuselage Integral Fuel Tank

The hydrodynamic ram effect is divided into three phases: the early shock phase, the later drag phase and the cavity phase [2].

Shock Phase: The shock phase is initiated when the projectile penetrates the wall of the tank and impacts the fluid. As the impact energy is transferred to the fluid, a hemispherical shock wave centered at the point of impact is formed. This creates an impulsive load on the inside of the entry wall in the vicinity of the entry hole causing the entry wall to crack and peel.

Drag Phase: As the projectile travels through the fluid, its kinetic energy is transformed into fluid motion as the projectile is slowed by viscous drag. A pressure field is generated as fluid is displaced from the projectile path. In contrast to the pressure field developed in the shock phase, the fluid is accelerated gradually rather than impulsively. The gradual acceleration causes the peak pressure to be much lower, and the duration of the pressure pulse to be longer.

Cavity Phase: During the drag phase, a radial velocity is imparted to the fluid and a cavity is formed behind the projectile. The subsequent expansion and collapse (oscillations) of the cavity constitutes the cavity phase of hydrodynamic ram. Significant pressure pulses can accompany the collapse of the cavity.

The structural response of the fuel tank walls to the hydrodynamic ram pressure is a complicated process. The pressure in the fluid caused by the high speed penetrating projectile loads the tank walls causing them to displace. This displacement in turn affects the pressure profile in the fluid, thus leading to a complex interaction between the fluid and the tank walls. This interaction phenomenon is referred to as fluid-structure interaction.

In this paper two issues of the hydrodynamic ram effect are addressed. In the first case, a parametric study is performed on a fluid filled tank structure penetrated by a high speed projectile. The following two parameters are varied for the first case:

1. Projectile Kinetic Energy
2. Fluid Density in the tank

These two parameters are varied and their effect on the structure, due to the hydrodynamic ram effect, is analyzed. Fluid pressure and displacements are measured and presented at the entry and exit points for all the various analytical cases and compared with one another.

In the second case, the projectile penetrates the fluid causing a hemispherical entry shock wave starting the hydrodynamic ram effect on the tank. Then the projectile explodes at a predetermined time within the tank. This explosion causes a blast wave to be generated. The combined effects of the blast wave and hydrodynamic ram effects are studied.

2. State of the Art in Hydrodynamic Ram Analysis

In the 1980's empirical codes such as ERAM and nonlinear analytical codes such as ABAQUS were coupled to give a complete hydrodynamic ram analysis. ERAM was used to determine hydrodynamic ram loads and ABAQUS was used as a nonlinear quasi-static analysis tool taking the peak pressures from ERAM. The problem with this method of performing the analysis was that the ERAM analysis method can only approximate fluid loads, and these loads are then simply used as applied loads in ABAQUS, ignoring the true coupling that actually occurs between the fluid and the structure.

ERAM is a digital computer code, which predicts the pressure and velocity throughout a rectangular volume of fluid due to a ballistic penetrator. A simplified model of the complex bullet behavior is used for the pressure computation. The rate of kinetic energy loss of the bullet is taken to be

$$\frac{dE}{dx_b} = m\beta V_b^2 \quad (1)$$

where E is the kinetic energy of the bullet, x_b is the bullet position, m is the bullet mass, V_b is the bullet velocity, and β is a velocity decay coefficient that is a function of x_b for the tumbling bullet. The wave equation is used to calculate the flow field resulting from the bullet and cavity motion. The source strength distribution is estimated by equating the energy loss of the bullet to the sum of the work done by the difference in ambient and cavity pressure and the kinetic energy of the fluid. The pressure in the fluid is computed using Bernoulli's equation.

$$P - P_o = -\rho\phi - \frac{\rho}{2}u^2 \quad (2)$$

where P is the fluid pressure, P_o is the ambient pressure, ρ is the fluid density, and ϕ is the velocity potential.

Using the method of images, reflections of the walls of the structure are also accounted for. The pressure due to the hydrodynamic ram effect is computed and transmitted to the ABAQUS model for structural response.

In the 1990's completely coupled fluid/structure interaction codes have been developed, including MSC/DYTRAN [3], ALE3D[4], and PRONTO-SPH. To perform the hydrodynamic ram analysis, a hydrocode should possess the following qualities.

1. Compressible and Incompressible Multi-Fluid Dynamics
2. Structural Dynamics
3. Detonation Physics
4. True Fluid/Structure Interaction
5. Advanced Constitutive Models (Large Strain Metal Plasticity/Failure, Composites)

6. Mixed Multi Materials

Features of MSC/DYTRAN are discussed in the next section. ALE3D is a research code from Lawrence Livermore National Laboratory to predict fluid-structure interaction. The main highlight of this code other than the normal hydrocode capabilities mentioned above is its mesh refinement capability for efficiency and accuracy in the Eulerian calculations. This mesh refinement technique is called grid relaxation. ALE3D employs a second order approximation for the fluid calculations involving the conservation of mass, momentum, and energy. The code lacks a good material model for composites and lacks failure capabilities for the structural model.

3. MSC/DYTRAN Model Description

The hydrodynamic ram analysis is performed on a fluid filled tank with, MSC/DYTRAN. MSC/DYTRAN is a three-dimensional analysis code for analyzing the dynamic, nonlinear behavior of solid components, structures, and fluids. It uses explicit time integration and incorporates features to simulate a wide range of material and geometric nonlinearity. The main characteristics of an explicit time integration scheme are:

1. Time step must relate to the shortest natural period of the mesh.
2. Time step size is set by the requirement to maintain stability in the explicit integration.
3. Mostly applicable in short time duration problems, such as wave propagation.

Explicit time integration is particularly suitable for analyzing short duration transient dynamic events that involve large deformation, a high degree of nonlinearity, and interaction between fluids and structures. MSC/DYTRAN couples a finite strain, large deflection structural finite element idealization (Lagrangian) with a finite volume fluid flow simulation (Eulerian). The Eulerian calculations, solve the Euler equations in integral form over a constant volume, conserving mass, momentum, and total energy at all time steps. The Eulerian equations in integral form over a volume are: Mass conservation (eq. 3), Momentum conservation (eq. 4), and Total Energy conservation (eq. 5)

$$\frac{\partial}{\partial t} \int_{vol} \rho dV = - \int_{surf} \rho u dS \quad (3)$$

$$\frac{\partial}{\partial t} \int_{vol} \int \rho u dV = - \int_{surf} \rho u u dS + \int_{surf} T dS \quad (4)$$

$$\frac{\partial}{\partial t} \iiint_{vol} \rho e dV = - \iint_{surf} \rho e u dS + \iint_{surf} u T dS \quad (5)$$

The physical variables P, ρ , u, e are transported from cell to cell during a time step.

In the simulations performed, the code was operated in both the Arbitrary Lagrange Euler (ALE) and general coupling mode. The general coupling mode allows for a arbitrary motion of structure through a fixed Eulerian domain. The Lagrangian structure presents a continuously moving flow boundary for the flowing material in the Eulerian mesh. While the flowing material in the Eulerian mesh simultaneously acts as a pressure load boundary on the Lagrangian structure.

In the ALE coupling approach, the Eulerian mesh does not remain fixed but is allowed to follow the motion of the Lagrangian mesh, since it is physically coupled to the Lagrangian mesh at the interface between the two. This means that at the interface between the fluid and the tank, the nodes at the boundary of the Eulerian mesh are attached to the nodes of the structural elements of the tank. Therefore, when the tank wall starts to move, the Euler mesh attached to the tank walls also starts to move. The fluid in the Eulerian elements adjacent to the tank wall then becomes compressed due to the motion of the wall, and exerts a pressure load back on the structural tank wall elements. To prevent highly distorted Eulerian elements at the interface between the Eulerian and Lagrangian meshes, a smoothing algorithm propagates the motion of the Eulerian mesh from the interface to the interior of the mesh.

The hydrodynamic ram model consists of two parts. A Lagrangian model for the tank (Figure 4) and an Eulerian model for the fluid inside the tank (Figure 5). The projectile is modeled as a rigid body, with the geometry defined by SURFACE cards. The dimensions of the tank and the projectile are shown in Figure 6.

The tank is a 36" x 36" x 36" cubical box modeled with four noded shell (CQUAD4) elements. The tank model consists of 1512 elements. The thickness of the tank walls is 0.125". SPCs are used to restrict movement of the tank at the bottom. The tank material is 2024-T3 aluminium and has been idealized as an ideal elastic plastic material.

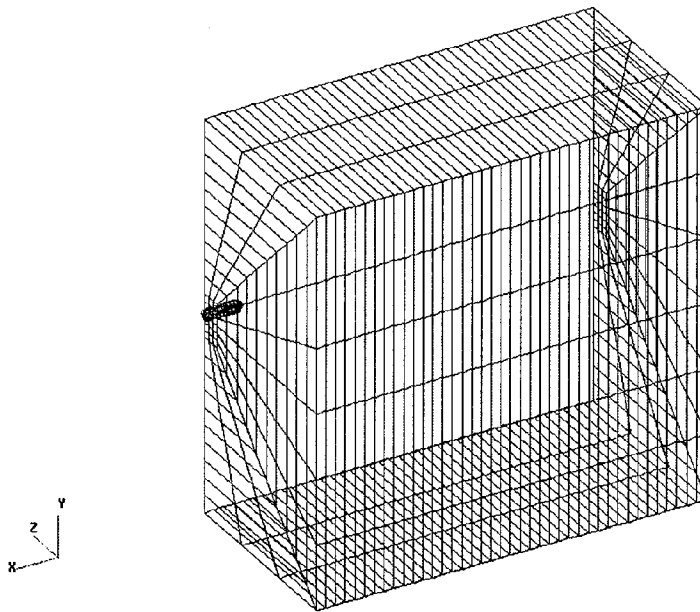
The water is modeled as an Eulerian hydrodynamic fluid with eight noded solid elements (CHEXA). The Eulerian model consists of 11040 elements. The penetration of the tank wall by the projectile is not modeled, but rather at the start of the analysis the projectile is placed flush with the inner wall as shown in. The projectile is 3.25" long with a 0.5" diameter, and is given an initial velocity at the start of the analysis. The entire analysis was run for 10 milliseconds.

For the second analysis case, the same model just described is used, except that the projectile is detonated inside the fluid, causing an explosive shock load. The explosive is detonated by a fuze delay. Principal features of the detonation are the formation of an expanding gas bubble con-

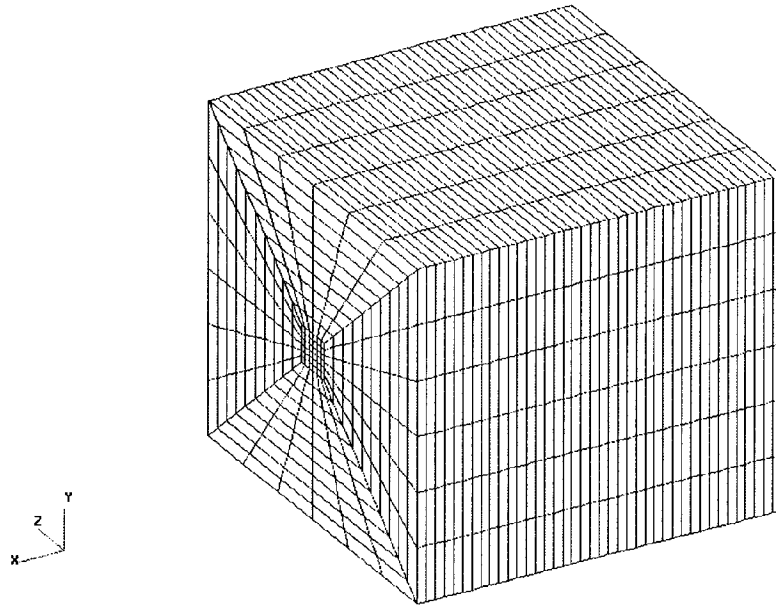
taining the gaseous detonation products (initially at very high pressure) then the progression of shock waves into the fluid from the expanding gas bubble. The tank walls are impulsively loaded through interaction with the propagating shock wave. The primary shock wave and interaction with the tank walls are the subject of this investigation.

Two types of fluid-structure interaction interfaces are invoked for this analysis:

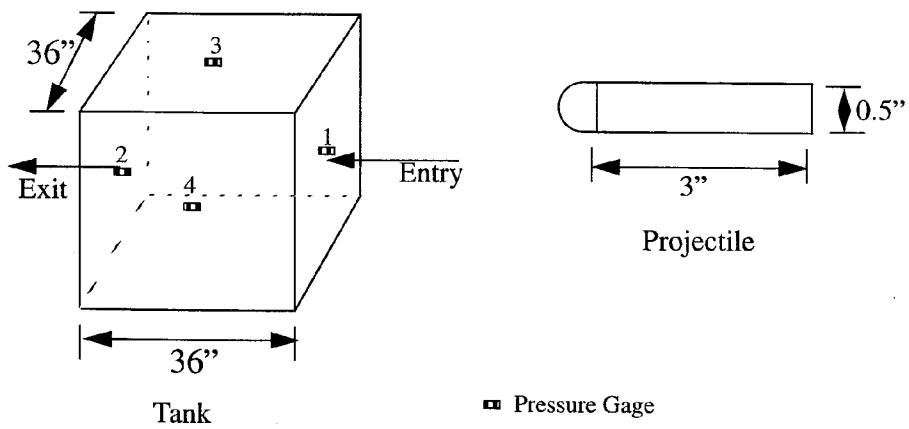
1. General Coupling: The projectile modeled as a rigid body is coupled to the Eulerian fluid inside the tank. This ensures the fluid-structure interaction between the moving projectile and the fluid.
2. Arbitrary Lagrange Euler (ALE) Coupling: The tank modeled as Lagrangian shell elements is coupled to the Eulerian fluid solid elements using the ALE technique. Forces and pressures generated in the fluid due to the projectile penetration and motion are transferred to the Lagrangian tank structure by the ALE interface.



4. Lagrangian Tank Model



5. Eulerian Fluid Model



6. Dimensions of the Tank and Projectile

4. MSC/DYTRAN Input Deck

An elastoplastic material was defined for the tank model. Aluminium 2024-T3 was defined as the tank material. A material failure model for the shell elements is defined using DMATEP and YLDVM cards. The failure criteria was defined in terms of equivalent plastic strain of the material. For the present analysis 70% plastic strain was considered failed.

The ALE coupling surface between the Lagrangian tank and Eulerian fluid model is defined with the ALE and ALEGRID cards.

Table 1. MSC/DYTRAN Sample Input Deck

Material Model for the Lagrangian Tank										
DMATEP	3	2.58E-4	10.5E6	0.33				1	100	
YLDVM	1	70.E3	10E4							
FAILMPS	100	0.07								
Definition of Fluid Inside the Tank (Water)										
PEULER1	999	2	HYDRO	1						
DMAT	2	9.35E-5	2							+
+		1.01								
EOSPOL	2	.319E6								
Initialization of the Fluid (Water)										
TICEL	1	10	DENSITY	9.35E-5						
SET1	10	10001	THRU	21040						
ALE Coupling between Tank and Fluid										
PSHELL	4		9999.							
SURFACE	107		SEG	4						
PSHELL	5	3	0.125							
SURFACE	800		PROP	123						
SET1	123	5								
ALE	17	800	107							

ALEGRID	75	0.								+
+	5001	THRU	24552							
General Coupling between Projectile and Fluid										
PSHELL	2	9999.								
COUPLE	88	66	INSIDE							
SURFACE	66		SEG	2						
Projectile Definition as Rigid										
RIGID	25	32	0.1		33.	18.	18.			+
+										+
+		5.								
SURFACE	32		PROP	101						
SET1	101	1								
PSHELL1	1		DUMMY							
Initialization of the Projectile										
TLOAD1	1	100		12						
FORCE	100	25		240000.	-1.0					

The Eulerian fluid model for water is defined by the EOSPOL, PEULER1, and the DMAT cards. The general coupling between the rigid projectile and the Eulerian fluid is defined with the COUPLE card. The projectile is defined with the RIGID and SURFACE cards. All the definitions of the above mentioned cards are shown in Table 1.

Table 2 shows the detonation setup for Case 2. The PEULER1 definition defines region in the Euler mesh with different materials (MMHYDRO). The JWL equation of state (EOSJWL) allows for the definition of the detonation time using the DETSPH card. Therefore one can program the explosion. To prevent premature ignition of the neighboring Eulerian elements due to advection of explosive material into them, a TIC is defined using TDET and set at $7.5E-4$ seconds (detonation time for the delayed explosive) for all the Eulerian elements (excluding the identified explosive Eulerian elements).

Table 2. MSC/DYTRAN Input Deck for Explosive Definition

Initialization of the Charge elements (HEI projectile)									
PEULER1	3		MMHYDRO	1					
TICEUL	1								+
+	ELEM	10	5	1	0.				+
+	ELEM	20	6	6	1.0				
DMAT	5	9.34E-5	2						+
+		1.1							
EOSPOL	2	.319E6							+
+	1.1								
TICVAL	4		DENSITY	9.34E-5	TDET	7.5E-4			
SET1	10	10001	THRU	20292					
SET1	10	20331	THRU	21040					
Definition of Explosive									
DMAT	6	1.48E-4	6						
EOSJWL	6	1.09E8	1.23E6	4.9	1.1	0.2			
Detonation Time is set to the time when the projectile reaches the center of the tank									
DETSPL	1	6	18.	19.	19.	2.9E5		7.5E-4	
TICVAL	5		DENSITY	1.12E-7	SIE	3.3E07			
SET1	20	20294	20293	20330	20329				

5. Parametric Study

A series of impact analysis into water-filled tanks were carried out to obtain data relevant to the hydrodynamic effect. Two parameters were varied. The velocity of the projectile and the density of the fluid inside the tank.

Case 1a: The velocity of the projectile was varied from 12,000 to 60,000 *in/sec* in increments of 12,000 *in/sec*.

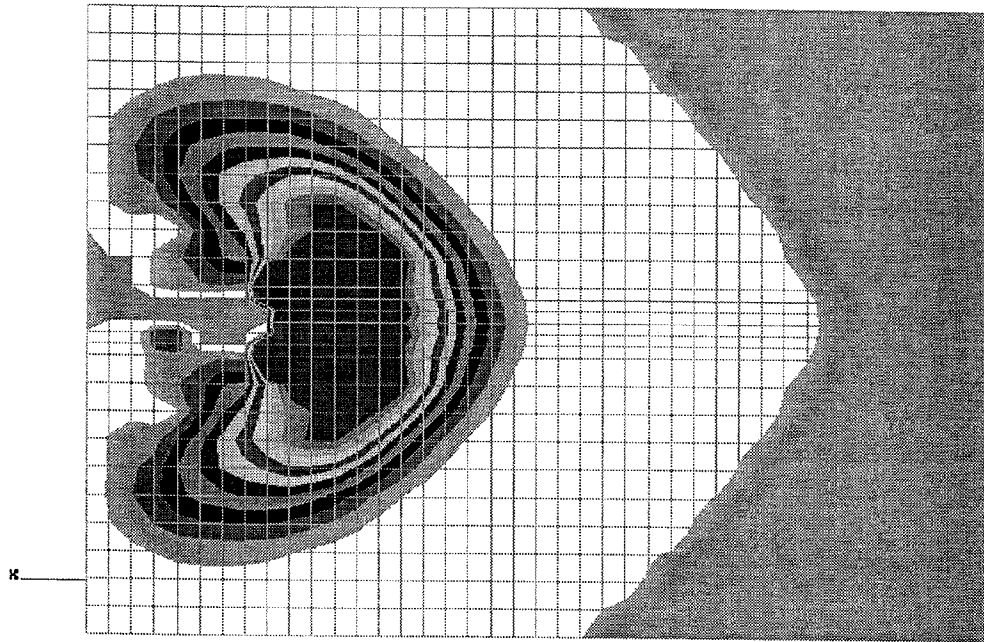
Case 1b: Three cases were studied for the fluid density variation. Half the density of water, density of water, and double the density of water.

Case 2: The effect of a projectile travelling at 24,000 *in/sec* through water and detonating at a pre-determined time and location in the tank is studied. The combined effect of the blast wave and the hydrodynamic ram is simulated.

Out of plane displacement and stress were obtained at the entrance and exit panels.

6. Results and Conclusions

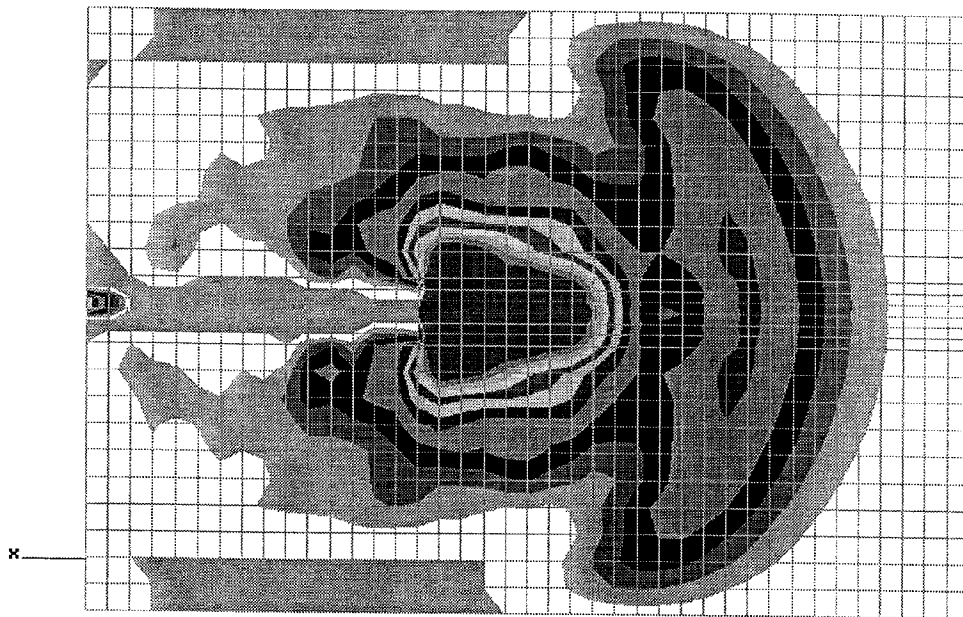
Hydrodynamic ram involves complicated dynamics and fluid/structure interaction. At the start of the analysis for the projectile travelling at 24,000 *in/sec*, a shock wave is created moving outward from the projectile as shown in Figure 7. In Figure 7 the trailing vacuum or drag phase is evident, and Figure 8 shows the eventual collapse of the cavity. Figure 9 shows the pressure and displacement time histories at the entry and exit panels for the 24,000 *in/sec* case study.



7. Shock and Drag Phase

At the exit plane a pressure reaction on the order of 20 *psi* occurs at 5.2E-4 seconds, while theoretically these nodes should remain at rest until approximately 6.0E-4 seconds. This is the time at which the bow shock would reach the exit panel (since the speed of sound in water is approximately 6.0E4 *in/sec*). The reason for the small pressure pulse seen at the exit panel even before

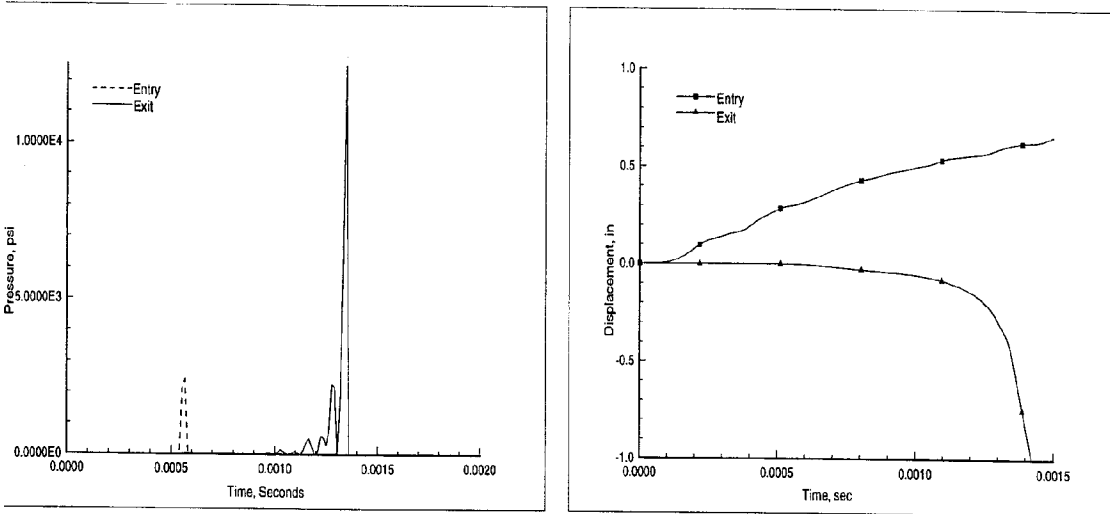
the projectile reaching, (Figure 9) is due to the pressure travelling through the wall of the aluminium tank. This pressure is due to the initial loading of the entry plane by the projectile, and arriving at the exit wall sooner than the fluid pressure since aluminium has a higher wave speed than water. The displacement time history (Figure 9) shows the displacement values at the entry and exit panels of the structure. From the sharp dip in the curve for the exit panel, it is clear that the projectile exits the panel around 1.4 E-3 seconds. This is about the right time that the projectile should reach the other end.



8. Cavity Phase and Collapse of Cavity

Since the projectile was flush mounted inside the entry panel, the entry panel does not show very high deformation. A maximum of 0.6 in was reached at the entry panel. From the exit panel curve which has a slight gradient, it is evident that displacement is felt in the exit panel even before the bow shock reaches the other end.

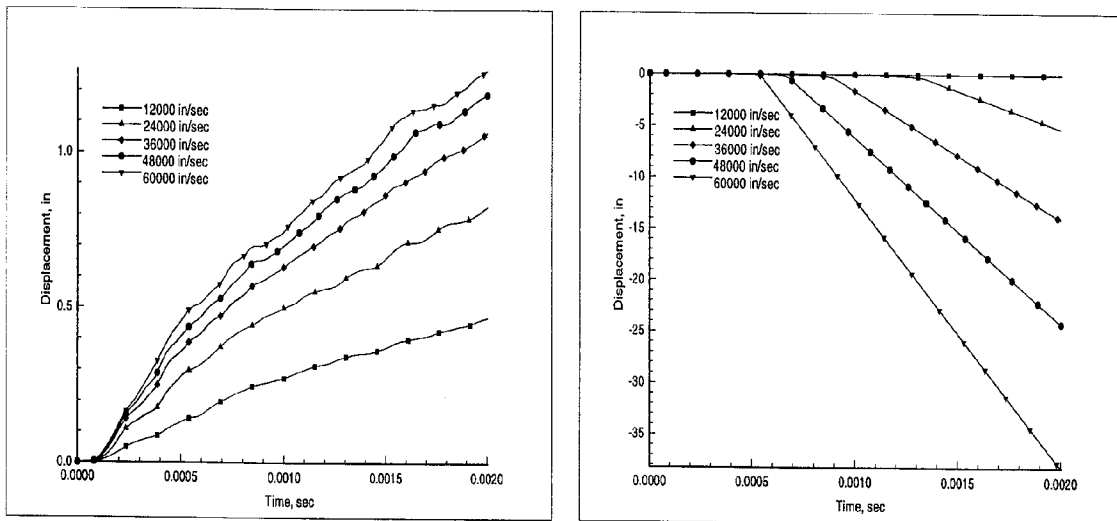
Hand calculations (Appendix A) were done to compare the entry and exit panel pressures using the equations described in section 2, and compared to those plotted in Figure 9 from MSC/DYTRAN. Detailed derivations for the calculation of pressure, displacement of the wall are given in Reference 5.



9. Pressure and Displacement Time History at the Entry and Exit Gages

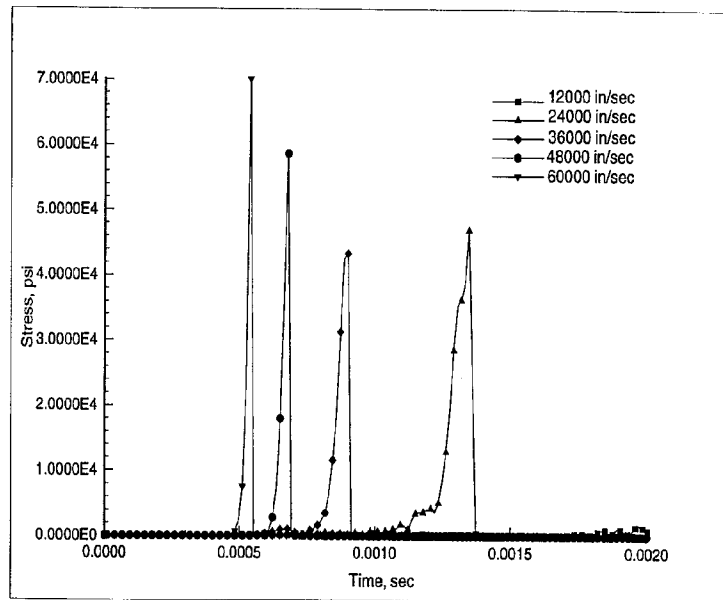
CASE 1a

In the case 1a study, the projectile velocity is varied from 12000 *in/sec* to 60000 *in/sec*. Figure 10 shows the displacement plots at the entry (left) and exit (right) panels. From the plots it is clear that there is a rapid increase in the displacement of the panels with the increase in projectile velocity. For the tank structure studied here, 24000 *in/sec* is the threshold velocity after which there is a sharp gradient in the displacement curve. The gradual dip in the exit displacement curve seen in Figure 9 (for the 24000 *in/sec* case), is not present for the 48000 *in/sec* and 60000 *in/sec* case.



10. Displacement at the Entry (left) and Exit (right) Panel for Case 1a

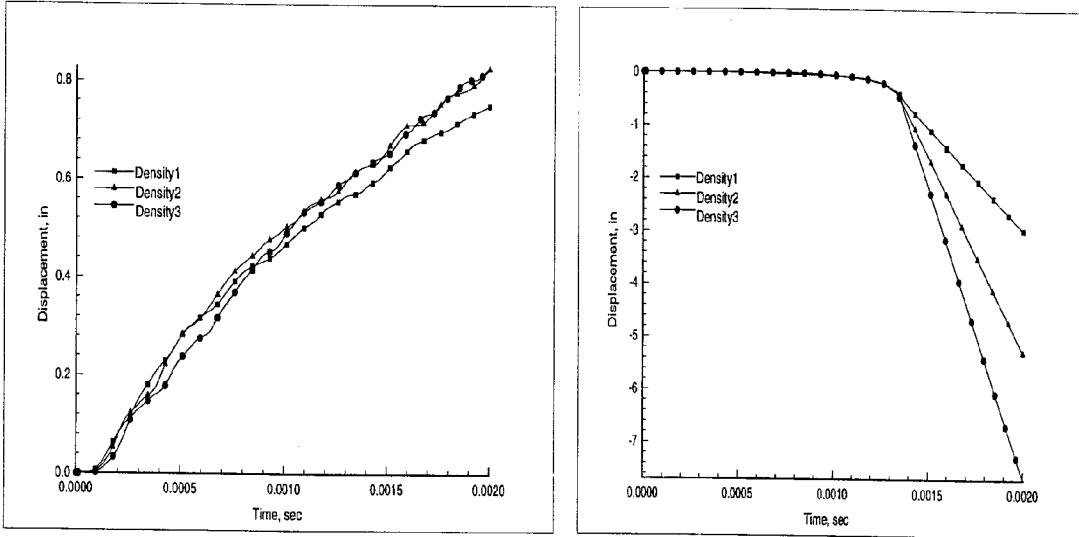
For the 60000 *in/sec* case, the velocity of the projectile and the velocity of the bow shock are about the same, therefore there is no gradual increase in the exit displacement plot (Figure 10). Figure 11 plot shows the stress vs. time plot for the five different velocities. At lower velocities the duration of the load application is much longer than those for the high velocity cases.



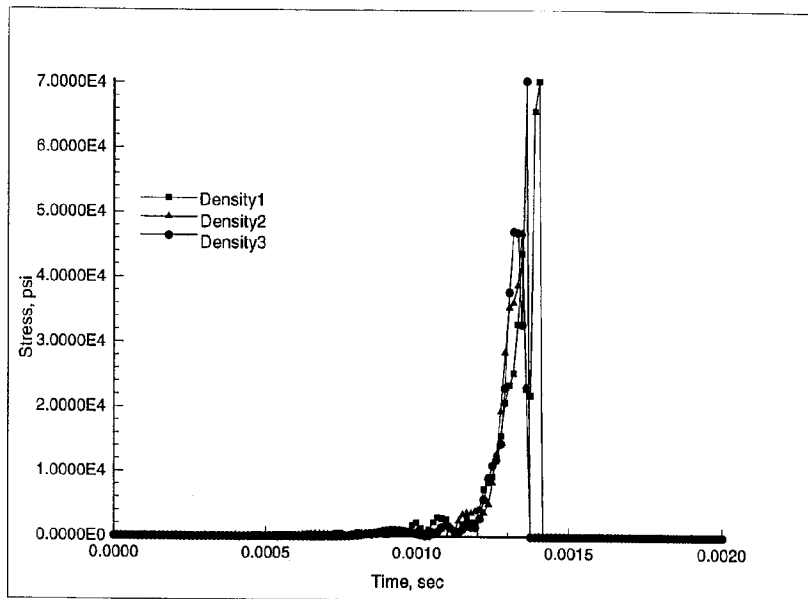
11. Stress at the Exit Panel for Case 1a

CASE 1b

In the case1b study, the projectile velocity is kept constant at 24000 *in/sec*, and the density of the fluid is varied from half the density of water, density of water, and double the density of water. Figure 12 shows the displacement plots at the entry (left) and exit (right) panels. Density1 = $4.67E-5 \text{ lbf} \cdot \text{s}^2/\text{in}^4$, Density2 = $9.35E-5 \text{ lbf} \cdot \text{s}^2/\text{in}^4$, and Density3 = $1.87E-4 \text{ lbf} \cdot \text{s}^2/\text{in}^4$. Figure 13 plots the stress levels at the exit panel. Examination of the data presented in Figure 12 and Figure 13 indicate that there is no discernible effect from the type of fuel used. There seems to be no consistent pattern of differences for this case studied. Further analysis need to be performed to come to definite conclusions.



12. Displacement and Stress/Strain at Entry and Exit Panels for Case 1b

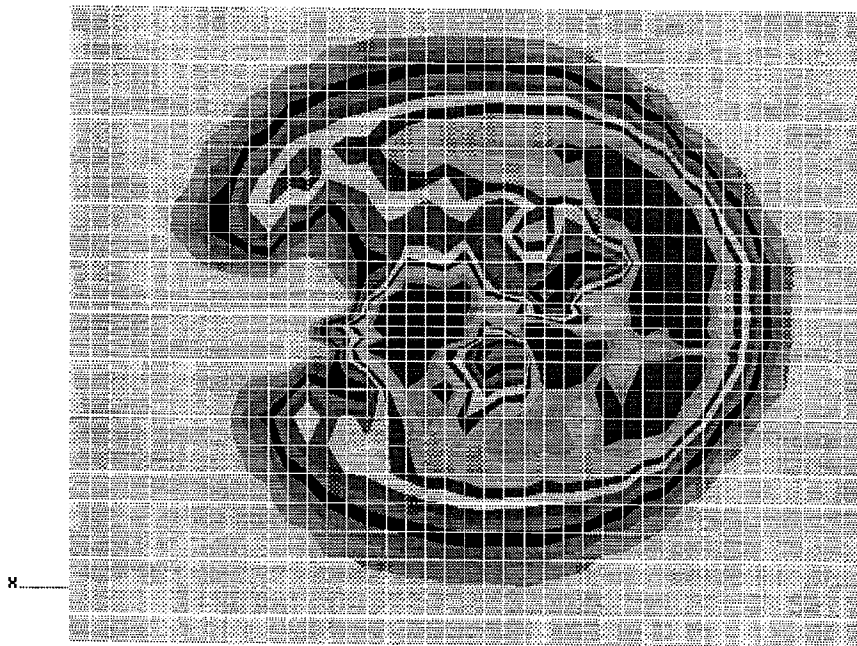


13. Stress at the Exit Panel for Case 1b

CASE 2

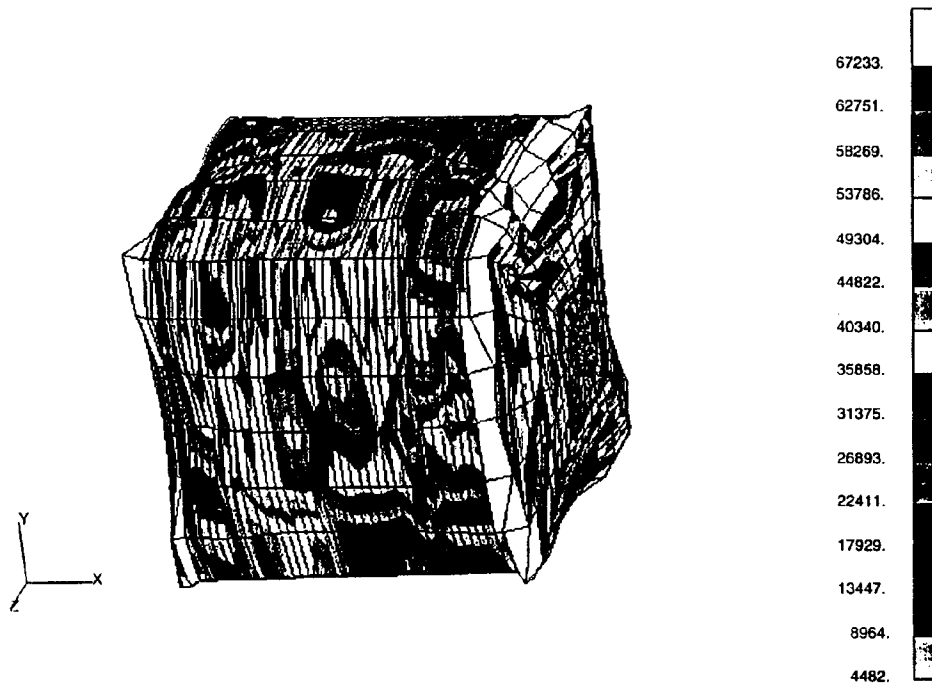
In this study the high velocity projectile, carrying a high explosive detonates by a fuzzy delay, at a predetermined time in the tank. This explosion causes a blast wave to be generated. The combined effects of the blast wave and the hydrodynamic effect due to the fluid is studied.

Figure 14 shows the pressure contours after charge detonation, forming a large sphere of 'C' shape. This shape is due to the vacuum trail where pressure build up is retarded since the trail first has to refill with water. The center region has pressure between 5600 and 700 *psi*, with a small peak up to 13000 *psi*. Figure 15 shows the deformation of the tank at 3 milliseconds.



14. Detonation of the Charge Inside the Tank

A proposed enhancement to MSC/DYTRAN to better simulate the hydrodynamic ram problem is to model the actual perforation of the tank walls, including failure of the elements at the tank wall entry point and venting of the fluid. The second important issue to be addressed is the layer by layer failure information on composites to determine the extent of damage due to the hydrodynamic ram effect. Appendix A compares MSC/DYTRAN predictions with empirical solutions.



15. Displacement of the Tank for Case2 at 3Milliseconds

References

1. Heitz, R.M., and Bischoff, G.H., "Small-Arms Fire Vulnerability and Protection of Aircraft Integral Fuel Tanks and Fuel Lines", Hydrodynamic Ram Seminar, Technical Report AFFDL-TR-77-32, May 1977.
2. Lee, T. W., "Preliminary Hydrodynamic Ram Investigations at Denver Research Institute", Hydrodynamic Ram Seminar, Technical Report AFFDL-TR-77-32, May 1977.
3. MSC/DYTRAN - A 3D Code for Explicit Transient Dynamics. The MacNeal-Schwendler Corporation, Los Angeles, CA.
4. ALE3D - An Arbitrary Lagrange/Eulerian 3D Code System, Lawrence Livermore National Laboratory.
5. Lundstrom, E.A., and Fung, W.K., "Fluid Dynamic Analysis of Hydraulic Ram IV", Report JTCG/AS-74-T-018, October 1976.

APPENDIX A

Bernoulli's equation yields,

$$P = P_o - \rho \frac{\partial \phi}{\partial t} - \frac{1}{2} \rho u^2 \quad (\text{A1})$$

where P = total fluid pressure, ρ = fluid density, ϕ = velocity potential, u = fluid velocity. In this calculation the u^2 term is neglected.

$$\frac{\partial \phi}{\partial t} = -\frac{1BA}{2R_b} \frac{V_b}{1 - \frac{V_b}{c} \frac{x - X_b}{R_b}} + \frac{1}{2} B^2 \ln \left(\frac{x + R_o}{x - X_b + R_b} \right) \quad (\text{A2})$$

where X_b = projectile position, R_b = distance between the projectile and the pressure measurement point, x = pressure point, R_o = distance between the impact point and the pressure point, V_b = velocity of the projectile, c = acoustic velocity in the fluid (60,000 in/sec).

$$B^2 = \frac{P_o - P_c}{\rho N} \quad (\text{A3})$$

where P_o = ambient pressure (14.7 psi), P_c = cavity pressure (assumed 0), N = Const. (2.99)

$$A^2 = \frac{\left(\frac{dE}{dx_b} \right)}{\pi (P_o - P_c)} \quad (\text{A4})$$

where E = Kinetic energy of the bullet (eq. 1). All the derivations of the above equations are given in Reference 5.

@Entry Panel: $X_b=12''$, $R_b=12''$, $x=0''$, $R_o=0''$, $B=229.30$, $A=111.68$ (for $\beta = 0.01$),
 $\rho = 9.35E-5 \text{ lbf} \cdot \text{s}^2/\text{in}^4$.

$$P_{\text{entry}} = 1780 \text{ psi}$$

@Exit Panel: $X_b=33''$, $R_b=3''$, $x=36''$, $R_o=36''$, $B=229.30$, $A=111.68$ (for $\beta = 0.01$),
 $\rho = 9.35E-5 \text{ lbf} \cdot \text{s}^2/\text{in}^4$.

$$P_{\text{exit}} = 15960 \text{ psi}$$

MSC/DYTRAN predicts $P_{\text{entry}} = 2800 \text{ psi}$ and $P_{\text{exit}} = 12200 \text{ psi}$